Sādhanā (2022) 47:269
https://doi.org/10.1007/s12046-022-02040-9

Application of response surface method for optimization of alkali activated slag concrete mix with used foundry sand as partial replacement of sand

NAGA RAJESH KANTA[1,2], MARKANDEYA RAJU PONNADA[3,*] and KAPILESWAR MISHRA[1]

[1]Department of Civil Engineering, Centurion University, Bhubaneswar, India
[2]Department of Civil Engineering, GMR Institute of Technology, Srikakulam, India
[3]Department of Civil Engineering, MVGR College of Engineering (A), Vizianagaram, India
e-mail: rajeshkanta@gmail.com; nagarajesh.k@gmrit.edu.in; markandeyaraju@yahoo.com; kapileswar.mishra@cutm.ac.in

MS received 31 March 2022; revised 8 September 2022; accepted 3 November 2022

Abstract. The present work is aimed to utilize slag as the primary source of binder (aluminosilicate) in alkali activated concrete so that CO_2 emissions can be reduced. Also, sand is partially replaced 20% by volume (constant) with Used Foundry Sand. Minitab's response surface method is applied to optimize the mixing proportions and also to study the effect of independent variables (Slag, Alkali/Binder and Fine aggregate/Coarse aggregate) on the dependent variables (compressive strength at 3, 7 and 28 days of curing). The experimental compressive strength of the studied concrete is measured and compared with the predicted results of the response surface method and the predictions are in good agreement. The optimized independent variables, S = 416.418 kg/m^3, A/B = 0.488 and F/C = 0.554 are also validated with another set of experiments and it is found that error is <10%. It can be concluded that Response Surface Method can be efficiently used in optimization.

Keywords. RSM; optimization; slag; used foundry sand; alkali activated slag concrete; compressive strength.

1. Introduction

In recent years, global climatic emergency assessment has been done by experts to estimate the emissions from the greenhouse effect and toxic contaminants. This is also done during the 2016 Paris agreement on climate change. Measures are aimed at mitigating global warming issues while promoting sustainable development [1–4]. As per Kyoto Protocol, for some countries, there are no specific targets for the reduction of greenhouse gas emissions and mitigation of toxic emissions. Broader targets need to be specified making it compulsory for the implementation of measures toward sustainable growth for all State Parties [5]. As per the agreement between the nations, it is the need of the hour to mitigate the carbon footprint and toxic pollutant emissions. Hence there is a huge demand for the utilization of green materials in concrete production as cement is the main source of carbon emissions in concrete [6]. The process of cement manufacturing involves calcination and combustion of clinker. Nearly a ton of cement emits one ton of CO_2. Due to this, there is an imperative need to look for alternatives of cement that require less heat energy but contains good amounts of CaO and/or also to make blended cement [7]. Today the present world is facing a major problem of a higher carbon footprint and increasing volumes of industrial waste. Both these problems can be addressed if industrial wastes are utilized as alternatives to cement and at the same time CO_2 emissions can also be handled smoothly [8]. The promising materials are slag, fly ash, bottom ash and silica fume which are byproducts of Iron and steel manufacturing plants. Recent research studies revealed that they can be used as alternatives to cement [9, 10]. Similarly, due to the depletion of natural sand deposits, many studies are done on the replacement with Used Foundry Sand, crusher dust, crushed limestone and marble dust [11, 12]. Studies conducted on the utilization of Used Foundry Sand (a byproduct of the foundry industry) at 20% give on par results compared to natural sand in concrete [13–16]. Currently, these industrial wastes are used as filling materials in embankments and soil strengthening. Utilization of these industrial wastes will also solve the problem of environmental hazards such as erosion, landslides and industrial solid waste management.

*For correspondence
Published online: 08 December 2022

Considerable research work on alkali activated concrete (AAC) has been done in the recent past. Results have been obtained in terms of mix proportioning, Alkali to Binder ratio (A/B), Fine aggregate to Coarse aggregate ratio (F/C), Sodium Silicate to Sodium Hydroxide ratio (Na_2SiO_3/NaOH), either binary or ternary blends of binders such as fly ash, ground granulated blast furnace slag (Slag), bottom ash and silica fume with or without cement [17]. However, existing research studies are conducted on simple multi-factor variate analysis for determining the optimum mix [18, 19]. The higher the F/C ratio (indicating the fine aggregate to coarse aggregate ratio), the better the packing density of all-in-aggregates due to lesser voids. This maximizes the density which in turn reduces the quantity of slag required and also helps in improving the engineering properties due to higher package density [20–23]. Compared to the conventional experimental works, the Response Surface Method (RSM) is a numerical computation modelling application that is also a subset of Design of Experiment (DOE). It is a popular tool and is one of the most widely used DOE methodologies compared to other methods like Taguchi, mixture, factorial and screening. Furthermore, RSM based model has various advantages such as a superior approach in anticipating the responses, the ability to build an accurate model with a small quantity of experimental data, reducing the number of trials required, evaluating the correlations between factors and comprehending the interaction effect of independent and dependent variables [24–26]. As per the understanding of authors from review of literatures, it can be summarized that there is little work done using RSM for blended cement concretes particularly with 100% replacement of cement by Slag and 20% replacement of sand by Used Foundry Sand. The aim of this work is to bridge this gap.

The objective of the current research work is to determine optimized mix proportions for concrete made by compeltely replacing cement with slag, partially replace the sand with Used Foundry Sand 20% by weight along with natural coarse aggregate and alkali activators prepared from pre-defined combinations of NaOH and Na_2SiO_3 using RSM. To optimize the mix ingredients such as Slag, A/B and F/C used in preparing Alkali Activated Slag Concrete for attaining the desired compressive strength Minitab software's Design of Experiment's application Response Surface Method is used. The novelty of the present work lies in combining experimental results and results from analytical analysis, as an alternative to complete experimental work to optimize the ingredients for which is more expensive and time consuming compared to the combined experimental and analytical work [27].

Further, the optimization results presented in this study are also different from those presented by earlier researchers who worked on RSM. Hence, the research significance of this work is that the statistical models for analytical analysis depend on experimental data but the advantage lies with the former being precise and accurate.

Further, using the analytical models, the prediction of output (responses) can be considered with a 95% confidence level for uncertainty in the strength assessment, thereby helping in producing an optimized and competent concrete mix [28–30].

2. Experimental program

2.1 *Materials*

The binder that is slag used in this study is obtained from the Visakhapatnam steel plant, India conforming to IS 455 [31], IS 10289 [32] and IS 16714 [33]. It is off white glassy structure with a specific gravity of 2.32 and the chemical composition is presented in table 1 which mainly constitutes CaO, SiO_2, Al_2O_3 and MgO. This is used as a primary source of aluminosilicate material for preparing alkali-activated slag concrete.

The river sand (fine aggregate) conforming to IS 2720 [34]; IS 2386 [35, 36] is brought from Nagavali river, Srikakulam, India. The sand specific gravity is 2.54 with a fineness modulus of 2.27. River sand is replaced with a constant 20% Used Foundry Sand (UFS) by weight. UFS conforming to IS 2720 [34]; IS 2386 [35, 36] is obtained from Sri Sai Ram Alloy Castings, Autonagar, Visakhapatnam, India. The specific gravity of UFS is 2.70 and the fineness modulus is 2.45. The Coarse Aggregate (CA) conforming IS 2720 [34]; IS 2386 [35, 36] is brought from a local retailer shop in Rajam, India. The nominal size of CA is 20 mm and 10 mm down with specific gravities of 2.66 and 2.7 respectively.

The alkaline activators used are solution combinations of sodium silicate (Na_2SiO_3) with Na_2O = 12%, SiO_2 = 30% and water = 57% and sodium hydroxide (NaOH) flakes of purity 98–99 to make 13 M solution. The chemicals are purchased from ASTRRA Chemicals, Chennai, India. The ratio of Na_2SiO_3 to NaOH is kept at 1.0 for the entire study [17]. The alkaline solution is prepared on the day of casting which helps in activate the slag that subsequently acts as a binder and contributes to the strength of Alkali Activated Slag Concrete [37, 38].

Table 1. Chemical composition of slag (%).

Elements	Slag (wt.) %
CaO	36.31
SiO_2	33.67
Al_2O_3	15.42
MgO	8.16
FeO	2.02
MnO	0.73

2.2 *Development of response surface model*

The RSM is one of the applications of numerical computation modelling and is also a subset of DOE, which follows the rule of statistical mathematics. RSM through DOE approach helps in reducing the number of experiments to be conducted, evaluating the relationships within the independent variables, understanding the interaction effect of independent and dependent variables and providing a numerical model based on the experimental output. Through generated numerical model, optimum results can be obtained. The model also predicts the output based on the derived numerical model [24, 25]. RSM is the most widely used tool in the research field due to its accuracy and less time consumption [39]. A software called Minitab is used in the present study to avoid the laborious calculations of mix design proportioning and optimization. So far, several optimization strategies have been employed in concrete technology research. Some researchers have claimed successful use of RSM in their study [40–42].

In the present RSM model, an experimental design method, Central Composite Design (CCD) which involves a two-level full factorial with cube points 8, midpoints in cube 4, axial points 6 and axial midpoints 2 is considered for a 3 factors design with one replicate and α equal to 1.633. The IVs (Independent Variables) and their levels of variation are shown in table 2. Based on the IVs, a 2^3 matrix (2 indicates the number of levels and 3 indicates the number of independent variables or factors) with 20 experimental runs given by face centred CCD is considered to assess the primary (linear), secondary (quadratic) and cross interaction of IVs and their effect on the Dependent Variables (DVs).

2.3 *Mix methodology and specimen preparation*

Due to a lack of codal provisions, the Alkali Activated Slag Concrete (AASC) mixing is followed based on the methodology proposed by [43–45]. According to the suggested 20 experimental runs, each mixed sample is prepared by mixing the IVs as shown in table 3. The prepared AASC mix is placed in cube moulds of size 150 mm × 150 mm × 150 mm and kept in ambient temperature curing. All the mixed specimens are covered with polythene sheets to avoid loss of moisture till the day of testing which is for 3, 7 and 28 days for measuring the responses in terms of compressive strength.

Table 2. Independent variables and their levels of variation.

		Levels of variation	
Independent variables	Symbols	Low	High
Slag (kg/m^3)	S	416	430
Alkali/binder*	A/B	0.46	0.49
Fine aggregate/coarse aggregate	F/C	0.53	0.59

* Binder represents slag

3. Results and discussion

3.1 *Compressive strength*

The compressive strength of all AASC hardened samples for 3, 7 and 28 days of curing are measured using the compression testing machine (capacity 2000 kN) under a controlled rate of loading 5.51 kN/s. It is anticipated that specimens with maximum slag content, A/B and F/C ratio will have higher compressive strength and similarly mixes with maximum slag content and maximum F/C ratio (mix M4) and maximum slag content with maximum A/B ratio (mix M5) will exhibit better compressive strength. The findings of this study revealed the same as shown in figure 1.

Even though mix M5 showed a higher initial 3 days compressive strength (which is abruptly higher than other mixes), consistent performance is observed in mix M11 and M4, due to higher slag and F/C. From table 3, the F/C for both M4 and M11 mixes is 0.59 indicating a densly packed well graded aggregate. The consistent increase in the compressive strength in M4 and M11 mixes is due to usage of densely packed well graded all-in-aggregates. It is inferred from table 4 that the 28 days strength variation of rest of mixes compared to M4 is in the range of 12.41–40.41%. From same table it is also observed 28 days strength variation of rest of mixes compared to M11 is in the range of 13.18–41.38%. [20, 46]. It is also considered that mix M4 is the optimal mix in the compressive strength aspect due to the lesser A/B ratio (0.46) and based on the fact that the higher the alkali content, the higher is the cost of the concrete production.

3.2 *RSM statistical analysis*

The significance and interaction of the IVs and their effect on the responses are determined using RSM statistical analysis and subsequent Analysis of Variance (ANOVA). The RSM responses are also expressed in the form of polynomial regression equations (Eqs. (1) to (3)) with R^2 = 86.71%, 83.40% and 85.48%, respectively. The experimental and predicted responses that are compressive strength (fck) at 3, 7 and 28 days of curing for various IVs are illustrated in table 4.

Table 3. 2^3 Matrix RSM-CCD suggested 20 runs with independent variables proportion.

Experimental run	Mix Id	S (kg/m^3)	A/B	F/C	Alkali (kg/m^3) Na_2SiO_3 (50%)	Alkali (kg/m^3) NaOH (50%)	Fine aggregate (kg/m^3) Sand (80%)	Fine aggregate (kg/m^3) UFS (20%)	Coarse aggregate (kg/m^3)
1	M1	416	0.46	0.53	95.68	95.68	535.06	133.76	1264.18
2	M2	423	0.475	0.56	100.46	100.46	534.4	133.6	1197.59
3	M3	423	0.475	0.56	100.46	100.46	534.4	133.6	1197.59
4	M4	430	0.46	0.59	98.9	98.9	534.4	133.6	1131
5	M5	430	0.49	0.53	105.35	105.35	535.06	133.76	1264.18
6	M6	416	0.49	0.59	101.92	101.92	534.4	133.6	1131
7	M7	416	0.49	0.53	101.92	101.92	535.06	133.76	1264.18
8	M8	416	0.46	0.59	95.68	95.68	534.4	133.6	1131
9	M9	423	0.475	0.56	100.46	100.46	534.4	133.6	1197.59
10	M10	430	0.46	0.53	98.9	98.9	535.06	133.76	1264.18
11	M11	430	0.49	0.59	105.35	105.35	534.4	133.6	1131
12	M12	423	0.475	0.56	100.46	100.46	534.4	133.6	1197.59
13	M13	423	0.475	0.609	100.46	100.46	534.4	133.6	1096.89
14	M14	423	0.475	0.511	100.46	100.46	534.4	133.6	1307.22
15	M15	423	0.499	0.56	105.64	105.64	534.4	133.6	1197.59
16	M16	423	0.475	0.56	100.46	100.46	534.4	133.6	1197.59
17	M17	411.57	0.475	0.56	97.75	97.747	534.4	133.6	1197.59
18	M18	423	0.475	0.56	100.46	100.46	534.4	133.6	1197.59
19	M19	434.43	0.475	0.56	103.17	103.17	534.4	133.6	1197.59
20	M20	423	0.451	0.56	95.28	95.28	534.4	133.6	1197.59

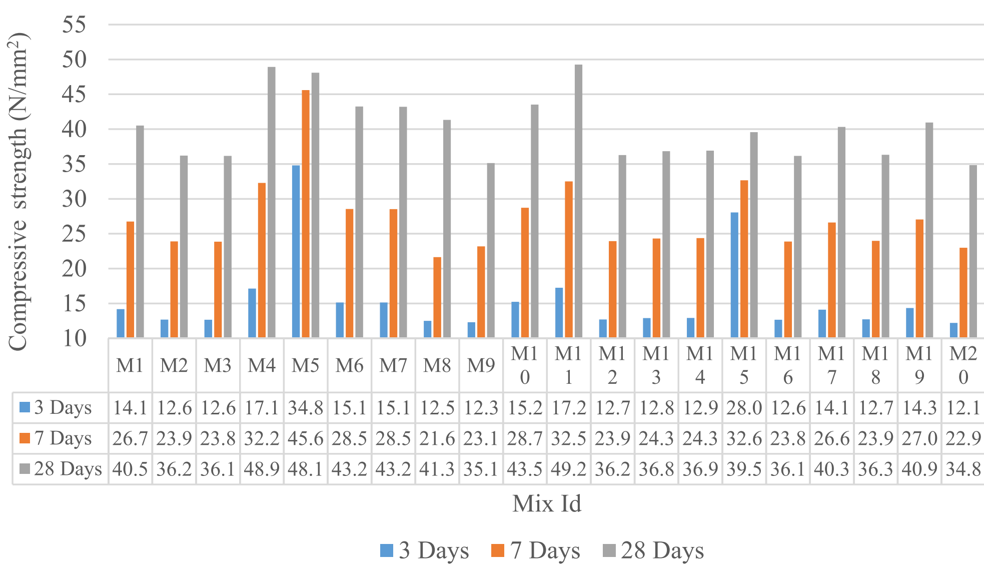

Figure 1. Compressive strength of all mixes.

$$fck3 = 7182 - 20.6S - 18478\left(\frac{A}{B}\right) + 14079\left(\frac{A}{B}\right)^2 \quad (1)$$

$$fck7 = 10590 - 38S - 13047\left(\frac{A}{B}\right) + 11044\left(\frac{A}{B}\right)^2 \quad (2)$$

$$fck28 = 14439 - 56.5S - 7203\left(\frac{A}{B}\right) - 2944\left(\frac{F}{C}\right) + 0.0646S^2 + 8333\left(\frac{A}{B}\right)^2 + 1948\left(\frac{F}{C}\right)^2 \quad (3)$$

Table 4. Compressive strength comparison of experimental and predicted using RSM.

Mix Id	Compressive Strength-fck (N/mm^2)								
	Experimental fck3,exp*	Predicted fck3,pre*	Ratio (fck3,exp/fck3,pre)	Experimental fck7,exp**	Predicted fck7,pre**	Ratio (fck7,exp/fck7,pre)	Experimental fck28,exp***	Predicted fck28,pre***	Ratio (fck28,exp/fck28,pre)
M1	14.18	12.86	1.10	26.74	26.01	1.03	40.52	41.06	0.99
M2	12.67	14.71	0.86	23.90	26.08	0.92	36.21	37.66	0.96
M3	12.66	14.71	0.86	23.87	26.08	0.92	36.16	37.66	0.96
M4	17.12	14.84	1.15	32.29	29.68	1.09	48.92	46.70	1.05
M5	34.80	32.35	1.08	45.60	41.91	1.09	48.10	46.85	1.03
M6	15.14	17.10	0.89	28.55	29.13	0.98	43.25	43.23	1.00
M7	15.12	17.07	0.89	28.52	29.36	0.97	43.21	44.08	0.98
M8	12.50	14.61	0.86	21.64	24.49	0.88	41.32	41.23	1.00
M9	12.30	11.13	1.11	23.19	22.34	1.04	35.14	36.93	0.95
M10	15.23	12.93	1.18	28.72	26.43	1.09	43.52	42.20	1.03
M11	17.24	18.22	0.95	32.51	31.50	1.03	49.26	47.38	1.04
M12	12.70	11.13	1.14	23.94	22.34	1.07	36.28	36.93	0.98
M13	12.89	11.03	1.17	24.31	22.78	1.07	36.83	38.77	0.95
M14	12.92	15.29	0.85	24.37	26.42	0.92	36.92	37.00	1.00
M15	28.06	26.40	1.06	32.67	33.45	0.98	39.56	40.32	0.98
M16	12.66	11.93	1.06	23.87	21.66	1.10	36.17	33.21	1.09
M17	14.11	11.07	1.27	26.61	22.86	1.16	40.32	38.89	1.04
M18	12.71	11.93	1.07	23.97	21.66	1.11	36.32	33.21	1.09
M19	14.34	17.88	0.80	27.03	31.24	0.87	40.96	44.41	0.92
M20	12.19	14.36	0.85	22.99	23.13	0.99	34.84	36.10	0.97

* fck3, exp and fck3, pre indicates experimental and predicted compressive strength of 3 days.

** fck7, exp and fck7, pre indicates experimental and predicted compressive strength of 7 days.

*** fck28, exp and fck28, pre indicates experimental and predicted compressive strength of 28 days.

The compressive strength (output) of various mixes is dependent on the weight of various model parameters (i.e., ingredients of concrete). For example, higher the cement content, higher the strength up to certain limit. Hence, it is understood that weight of each of the ingredients of constituents are most influencing parameters on the output i.e., Compressive strength in this case. Further, in the manuscript, the comparison is also presented for coefficients of the influencing model parameters. The coefficients of model parameters/terms are weights attached to each of the parameters to obtain a required compressive strength. For example, the influence of A/B ratio on compressive strength may be higher than the other parameters. Hence, the coefficients are compared in the study to compare the influence of each parameter on the output i.e., Compressive strength. The two comparisons discussed are two different aspects. The former is to obtain the optimum mix proportions and the later is to understand the weightage of each parameter on the required compressive strength of concrete. ANOVA results of various IVs along with their p value and significance are given in table 5. Based on table 5, it is observed that terms with $p \leq 0.05$ are considered as significant and whereas $p > 0.05$ are considered as insignificant. The insignificant terms are eliminated from the second-order polynomial regression Eqs. (1) to (3). It is inferred from Eqs. (1) to (3) and table 5, in the second-order polynomial Eq. (1), the linear and square terms of (A/B) are considered the most influential terms due to their p values 0.003 and 0.007 respectively. In the same equation, even though the linear term (S) is having less influence due to its p value 0.046 close to 0.05, but to maintain hierarchy (S) term is provided. In Eq. (2), the most influential are linear terms (S) and (A/B) with p values 0.027 and 0.01 respectively and square term (A/B) with a p value 0.031. It is observed from Eq. (3) that only square terms are influential among which the p value for a square term (S) is 0.003 considered highly influential than the remaining square terms. To maintain the hierarchy, the linear terms S, (A/B) and (F/C) are incorporated in Eq. (3), even though they are insignificant. According to the studies reported by Soto, Cibilakshmi and Habibi, the higher the coefficients of the terms in the equations the higher the significance of the strength prediction and vice versa [40, 47, 48]. The 3, 7 and 28 days compressive strength of mix M4 exhibited consistent increase compared to all other mixes experimental result, it is due to maximum slag and maximum (F/C). On the other hand, even though ANOVA prediction results of mix M4 is consistently increased but marginal reduction in strength is observed due to insignificance of (F/C) in Eqs. (1) and (2). The 3 and 7 days experimental and

Table 5. ANOVA results of regression model.

	Compressive Strength (fck) N/mm^2					
	3 days		7 days		28 days	
Term	*p* Value	Significance	*p* Value	Significance	*p* Value	Significance
S	0.046	Yes	0.027	Yes	0.053	No
A/B	0.003	Yes	0.010	Yes	0.121	No
F/C	0.178	No	0.273	No	0.486	No
S^2	0.313	No	0.066	No	0.003	Yes
(A/B)^2	0.007	Yes	0.031	Yes	0.037	Yes
(F/C)^2	0.618	No	0.280	No	0.047	Yes
S × (A/B)	0.115	No	0.368	No	0.970	No
S × (F/C)	0.163	No	0.595	No	0.478	No
(A/B) × (F/C)	0.087	No	0.241	No	0.534	No

prediction compressive strength ratio of mix M4 is only 1.15 and 1.09 respectively, it indicates experimental and prediction results are in good agreement.

Based on the ANOVA results, it is also clear that there is no cross interaction between the IVs and it is evident that the cross interactions are statistically insignificant on the DVs, thereby they are not considered in the prediction model equations.

The ordinary least squares method considered in Minitab software is used to estimate unknown parameters in a model. In other words, it is used to find the best fit line for the data points. The method relies on reducing the sum of squared residuals between predicted and actual values. The discrepancy between the actual and predicted values is known as the residual which is also termed an error. The residuals are plotted on a normal probability graph to assess their normal distribution and linearity. A normal probability chart is a graphic illustration used to assess data distribution and establish its sufficiency. It is a scatter plot of residuals, the diagonal line passing through the data points is considered the best fit line and also helps in assessing the relationship between the experiment and predicted values. From figure 2, it is observed that most of the residuals of 3, 7 and 28 days are rationally lying close to the straight line indicating a linear relationship and that data is normally distributed [48, 49].

3.3 *Surface plots for 3, 7 and 28 days compressive strength (fck)*

The trend in variation and influence of Independent Variables (IVs) on the Dependent Variables (DVs) can be understood with 3D surface plots shown in figures 3, 4 and 5. From these figures, all the responses (compressive strength, fck at 3, 7 and 28 days) are plotted on the Z-axis, whereas the IVs are plotted on the X and Y-axes. The surface plots are drawn as a function of two IVs while holding the third IV value.

Figure 3a presents the surface plot between S on the X-axis and (A/B) on Y-axis. From figure 3a it is clear that due to the high significance of (A/B), higher strength is observed. Further, S is contributing moderately to strength by holding the (F/C) at 0.56 which is insignificant. It is inferred that at maximum slag content of 430 kg/m^3 and maximum A/B of 0.5, 3 days compressive strength is approximately 38 N/mm^2. This is due to the improved alkali activation in the mix. From figure 3b, it is evident that (F/C) is not contributing to the strength due to its insignificance. Hence a negligible compressive strength (i.e., <15 N/mm^2) is reported even though (A/B) is holding at 0.475 which is highly significant. On the other side, with S varying from 410 to 430 kg/m^3 and (A/B) holding at 0.475, an increase in strength from 10 to 25 N/mm^2 is observed. This moderate strength is due to a moderate quantity of alkali concentration. From figure 3c, it is also clear that due to the insignificance of (F/C), strength is not influenced by that term and is negligible <10 N/mm^2. From the same figure, it is evident that for (A/B) ranging from 0.45 to 0.50 and S holding at 423 kg/m^3, an increasing trend in strength is observed from 10 to 40 N/mm^2. This increment in strength resulted because of an increased quantity of alkali concentration.

The 7 days compressive strength has followed a similar trend of 3 days strength which is evident from Eq. (2) and figure 4. From figure 4a, it is evident that S contributes moderate strength due to its moderate significance and with (A/B) due to its higher significance contributed greatly to strength increment by holding (F/C) at 0.56 which is insignificant. It is inferred that the 7 days compressive strength of AASC with slag content 430 kg/m^3 (maximum) and A/B ratio of 0.5 (maximum) resulted in compressive strength of approximately 48 N/mm^2 due to high alkali activation. It is observed from figure 4b that (F/C) is not contributing to the strength due to its insignificance. From

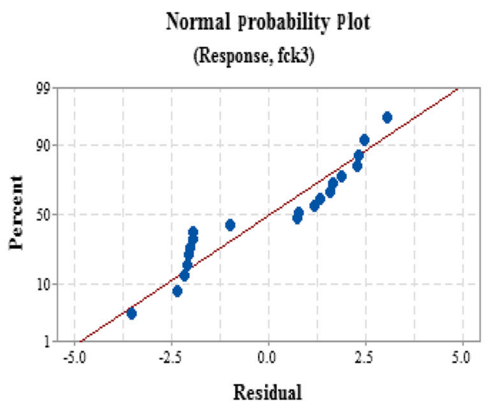

(**a**) Normal probability plot - residual at 3 days.

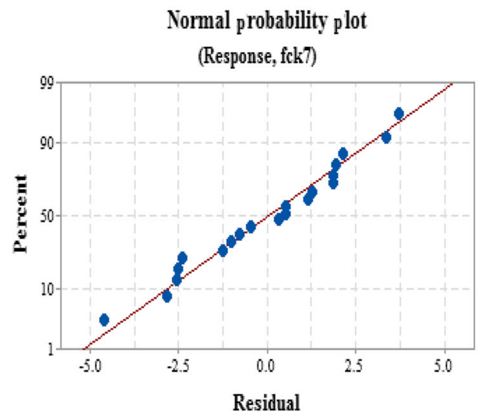

(**b**) Normal probability plot - residual at 7 days.

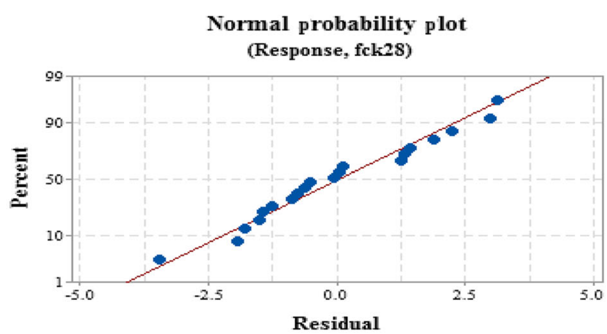

(**c**) Normal probability plot - residual at 28 days.

Figure 2. Normal probability plots—residuals (3, 7 and 28 days).

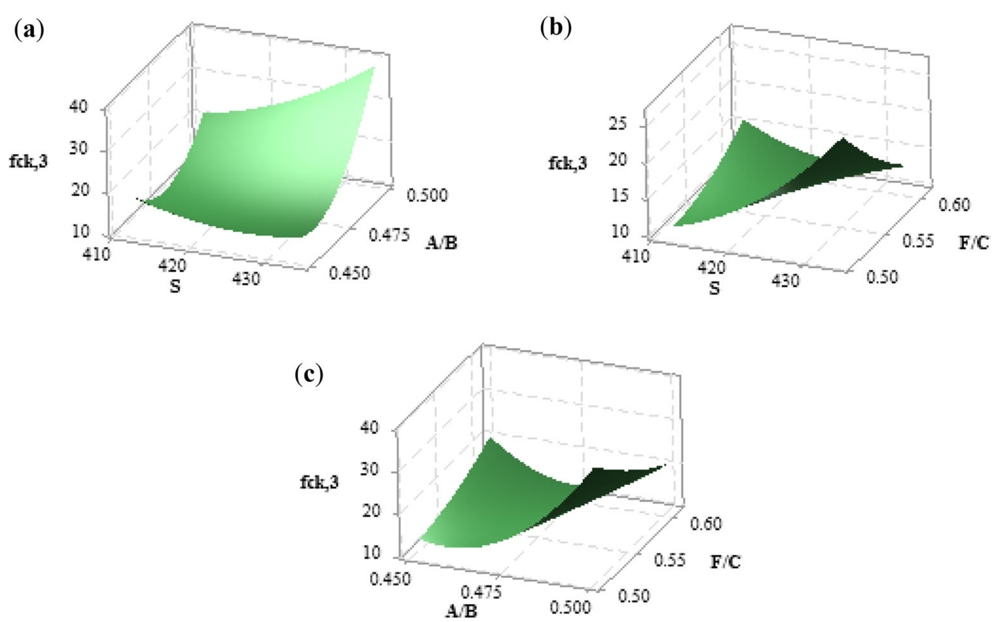

Figure 3. Surface plots of 3 days compressive strength with various IVs on X and Y axes.

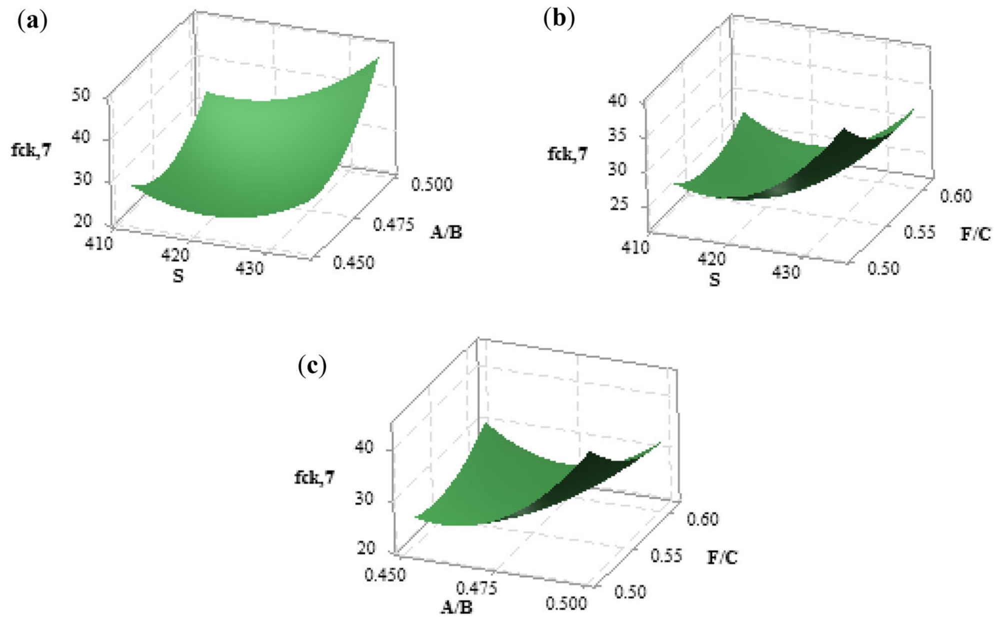

Figure 4. Surface plots of 7 days compressive strength with various IVs on X and Y axes.

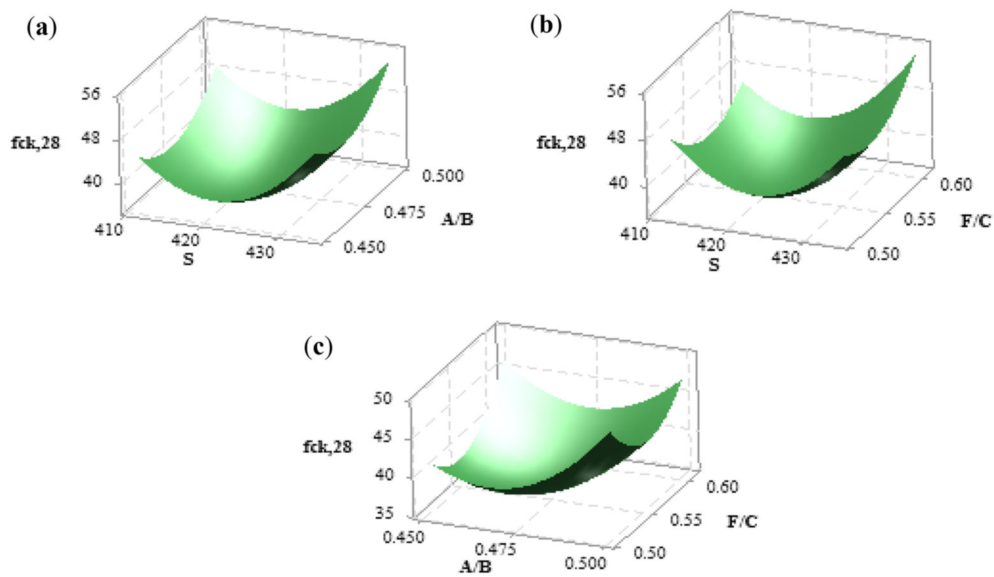

Figure 5. Surface plots of 28 days compressive strength with various IVs on X and Y axes.

the same figure, with S varying from 410 to 430 kg/m^3 and by holding (A/B) at a moderate value of 0.475, an increasing trend in strength from 25 to 40 N/mm^2 is observed. This is due to the high significance of (A/B) leading to improved alkali activation in the mix. It is inferred from figure 4c that, due to the insignificance of (F/C), strength is not influenced. With S holding at 423 kg/m^3 and highly significant term (A/B) ranging from 0.45 to 0.50 showed an increasing trend in strength from 20 to 40 N/mm^2 is observed. This is due to an increment in the quantity of alkali concentration.

In figure 5, even though linear terms S, (A/B) and (F/C) are insignificant, the square terms of the same are highly significant and contributed to variation in strength. In figure 5a, the surface plot is drawn with S, (A/B) and 28 days response (fck,28) represented on X, Y and Z axes respectively while holding (F/C) at 0.56. It can be concluded that an increase in slag content from 410 to 420 kg/m^3 resulted in a decreased trend in 28 days compressive strength approximately from 48 N/mm^2 to about 40 N/mm^2. This is because of the insignificance of the linear terms. But reported strength due to square terms is significant which indicates their influence. Further increment in slag to 430 kg/m^3 showed an increased trend in 28 days compressive strength approximately up to 48 N/mm^2. Figure 5b is a plot with S, (F/C) and fck,28 on X, Y and Z axes respectively, by holding (A/B) moderately at 0.475. From the same figure, with an increase in slag content from 410 to 420 kg/m^3, a decreasing trend in 28 days compressive strength is observed approximately from 48 N/mm^2 to about 40 N/mm^2. It is evident that it has followed a similar trend to figure 5a. On the other hand, varying (F/C) from 0.53 to 0.59 resulted in a strength of 44 N/mm^2 due to the significance of square terms. Figure 5c is a plot with (A/B), (F/C) and fck,28 on the X, Y and Z axes respectively by holding S moderately at 423 kg/m^3. From figure 5c, it is inferred that the increment of A/B from 0.45 to 0.475, shows a slightly decreased trend in 28 days compressive strength approximately from 40 to 38 N/mm^2. A further increment in A/B to 0.50 resulted in 28 days compressive strength of approximately 48 N/mm^2. The increment in strength is observed due to the significance of square terms (A/B) and (F/C) indicating that high alkali activation and dense particle packing respectively are responsible for improved strength.

3.4 *Optimization of mix*

In RSM, D-optimal is used to optimize the AASC mix proportions. Table 6 shows the criteria to produce the greatest possible compressive strength at 3, 7 and 28 days of curing. For this from table 4, desired target compressive strength for various curing days is fixed in between the lower and upper values of experimental compressive strength at various curing days. The optimized compressive strength for 3, 7 and 28 days of curing for optimum IVs setting at S = 416 kg/m^3, A/B = 0.488 and F/C = 0.55 are 16, 27 and 40 N/mm^2 and the same are shown in figure 6. The representations 'y' and 'd' indicate maximum compressive strength at various curing days and desirability of IVs respectively. The range of 'd' varies from 1 to 0, indicating most desirable and undesirable respectively. From figure 6, the optimal composite desirability is d = 0.98 which is attained with response desirability at d = 0.99 for 3 and 28 days compressive strength and d = 0.96 for 7 days compressive strength which indicates that the optimal IVs as per table 6 are most desirable for all curing days.

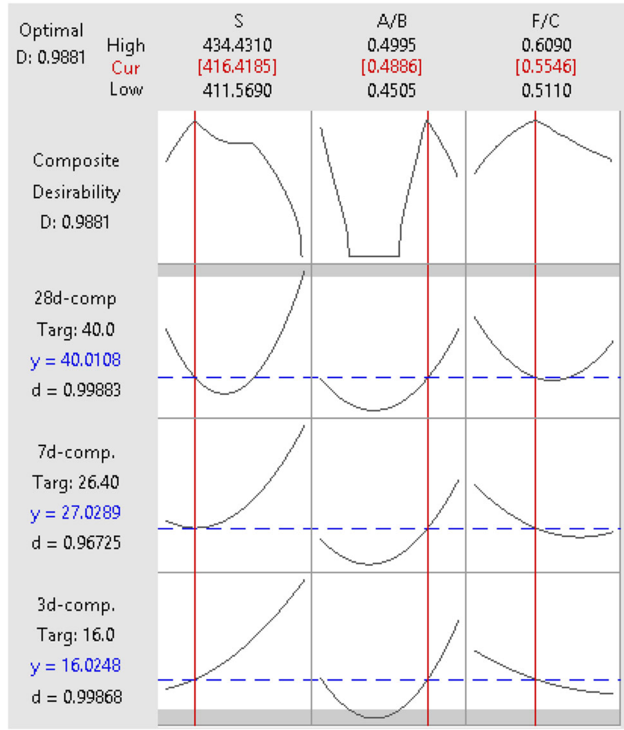

Figure 6. Optimization plots of RSM for target compressive strengths at 3, 7 and 28 days of curing.

3.5 *Validation of models*

The validation of the model is done by conducting the experiment analysis based on the optimized quantities of IVs (S = 416.418 kg/m^3, A/B = 0.488 and F/C = 0.554) shown in figure 6. The model predicted and experimental results are shown in table 7 are compared along with error percent. It is inferred that error percent <10%, indicates that RSM could predict and also optimize the quantities of materials, time, resources and responses with good accuracy.

Table 6. Criteria's for optimization of independent variables.

	Measured responses (N/mm^2)		Optimization	
Dependent variables (fck)	Lower	Upper	Goal	Target (N/mm^2)
3 days compressive strength	12.194	34.80	Target	16.0
7 days compressive strength	21.640	45.60	Target	26.4
28 days compressive strength	34.840	49.26	Target	40.0

Table 7. Validation of RSM and experimental results.

Optimized independent variables	3 days compressive strength (N/mm^2)			7 days compressive strength (N/mm^2)			28 days compressive strength (N/mm^2)		
	RSM, predicted	Experimental measured	Error percent	RSM, predicted	Experimental measured	Error percent	RSM, predicted	Experimental measured	Error percent
S = 416.418 kg/m^3 A/B = 0.488 F/C = 0.554	16.02	17.62	9.12	27.02	28.73	5.95	40.00	42.98	6.92

4. Conclusions

The following conclusions are drawn based on the attempt made to optimize the AASC mix proportions with RSM, the effect of independent variables such as Slag, Alkali to Binder ratio and Fine aggregate to Coarse aggregate ratio are analyzed and the results in terms of optimization of mixing ingredients and maximum gain in compressive strength are presented.

- Portland cement replaced with 100% Slag is found to be beneficial in compressive strength aspects at 3, 7 and 28 days of curing.
- Used Foundry Sand (20% by volume) can effectively replace the sand, due to the efficient performance of AASC in compressive strength aspects at 3, 7 and 28 days of curing.
- RSM statistical analysis is found to be an effective tool for analyzing the influence of independent variables on the responses (compressive strength at 3, 7 and 28 days of curing) of AASC.
- It can be concluded from the ANOVA and normal probability analysis of independent and dependent variables that they support the method of least squares fit. This is because the *p* values of independent variables are $\leq$0.05 and R^2 prediction of dependent variables (compressive strength) are 86.71%, 83.40% and 85.48% for 3, 7 and 28 days, respectively.
- Based on ANOVA results, there is no cross interaction is observed between the independent variables.
- From the ANOVA regression analysis, it is inferred that the most significant independent variable is the square term A/B (0.50) which contributes to the better 28 days compressive strength (approximately 53 N/mm^2) of AASC.
- Based on RSM's D-Optimal, the optimized independent variables, S = 416.418 kg/m^3, A/B = 0.488 and F/C = 0.554 are validated with experiment and found that error <10% indicates that the RSM can be effectively utilized in the prediction, optimization of mixing ingredients and resources with good accuracy in strength assessment.

Acknowledgements

The authors sincerely acknowledge the MINITAB Team for providing the trail version, which is used in this work and also other colleagues who gave moral support. No funding was received for this work.

Declarations

Competing interests The authors have no relevant financial or non-financial interests to disclose.

References

[1] UNFCCC 2016 *Climate Action Now-Summary for Policy-makers. United Nations Climate Change Secretariat*. Retrieved from climateaction2020.unfccc.int

[2] UNFCCC 2018 *Climate Action Now. Climate Action Now: Summary for Policymakers 2018*

[3] Lakshmanan P K, Singh S and Asta Lakshmi S 2017 The Paris agreement on climate change and India. *Journal of Climate Change* 3(1): 1–10. https://doi.org/10.3233/jcc-170001

[4] Intergovernmental Panel on Climate Change 2014 *Climate Change 2014 Mitigation of Climate Change. Climate Change 2014 Mitigation of Climate Change*. https://doi.org/10.1017/cbo9781107415416

[5] United Nations Climate Change 2019 What is the Kyoto Protocol? *United Nations Climate Change*, 1–6. Retrieved from https://unfccc.int/process-and-meetings/the-kyoto-protocol/what-is-the-kyoto-protocol/what-is-the-kyoto-protocol

[6] Rajesh K N, Raju P M, Mishra K and Madisetti P K 2021 A review on sustainable concrete mix proportions. *IOP Conference Series: Materials Science and Engineering* 1025: 012019. https://doi.org/10.1088/1757-899x/1025/1/012019

[7] van Oss H G 2005 *Background Facts and Issues Concerning Cement and Cement Data*. Retrieved from http://www.usgs.gov

[8] Poinot T, Laracy M E, Aponte C, Jennings H M, Ochsendorf J A and Olivetti E A 2018 Beneficial use of boiler ash in alkali-activated bricks. *Resources, Conservation and Recycling*. https://doi.org/10.1016/j.resconrec.2017.09.013

[9] Marinkovic S and Dragas J 2018 Fly ash. In: *Waste and Supplementary Cementitious Materials in Concrete* (eds)

Siddique R and Cachim P, Elsevier, Amsterdam. https://doi.org/10.1016/B978-0-08-102156-9.00011-0

[10] Yuksel I 2018 Blast-furnace slag. In: *Waste and Supplementary Cementitious Materials in Concrete: Characterisation, Properties and Applications* (eds) Siddique R and Cachim P, Elsevier, London, pp 361–415. https://doi.org/10.1016/B978-0-08-102156-9.00012-2

[11] Al-mashhadani M M and Canpolat O 2020 Effect of various NaOH molarities and various filling materials on the behavior of fly ash based geopolymer composites. *Construction and Building Materials*. https://doi.org/10.1016/j.conbuildmat.2020.120560

[12] Mavroulidou M and Lawrence D 2019 Can waste foundry sand fully replace structural concrete sand? *Journal of Material Cycles and Waste Management*. https://doi.org/10.1007/s10163-018-00821-1

[13] Bhardwaj B and Kumar P 2018 Effect of waste foundry sand addition on strength, permeability and microstructure of ambient cured geopolymer concrete. *IOP Conference Series: Materials Science and Engineering*. https://doi.org/10.1088/1757-899X/431/9/092009

[14] Bhardwaj B and Kumar P 2017 Waste foundry sand in concrete: a review. *Construction and Building Materials* 156: 661–674. https://doi.org/10.1016/j.conbuildmat.2017.09.010

[15] Tittarelli F 2018 Waste foundry sand. In: *Waste and Supplementary Cementitious Materials in Concrete: Characterisation, Properties and Applications* (eds) Siddique R and Cachim P, Elsevier, London, pp 121–147. https://doi.org/10.1016/B978-0-08-102156-9.00004-3

[16] Torres A, Bartlett L and Pilgrim C 2017 Effect of foundry waste on the mechanical properties of portland cement concrete. *Construction and Building Materials*. https://doi.org/10.1016/j.conbuildmat.2017.01.028

[17] Patankar S V, Ghugal Y M and Jamkar S S 2015 Mix design of fly ash based geopolymer concrete. In: *Springer India Advances in Structural Engineering (Materials)* (ed) Matsagar V, Springer India, New Delhi. https://doi.org/10.1007/978-81-322-2187-6

[18] Sun Q, Zhu H, Li H, Zhu H and Gao M 2018 Application of response surface methodology in the optimization of fly ash geopolymer concrete. *ISA Transactions.* 48: 45–52

[19] Ramkumar B G, Barmavath S and Nagaraju K 2017 Application of response surface methodology for optimization of alkali activated slag concrete. *International Journal of Scientific Development and Research*, *2*(3): 35–47. Retrieved from www.ijsdr.org

[20] Thunuguntla C S and Gunneswara Rao T D 2018 Mix design procedure for alkali-activated slag concrete using particle packing theory. *Journal of Materials in Civil Engineering*. https://doi.org/10.1061/(asce)mt.1943-5533.0002296

[21] Borges P H R, Fonseca L F, Nunes V A, Panzera T H and Martuscelli C C 2014 Andreasen particle packing method on the development of geopolymer concrete for civil engineering. *Journal of Materials in Civil Engineering*. https://doi.org/10.1061/(asce)mt.1943-5533.0000838

[22] Joseph B and Mathew G 2012 Influence of aggregate content on the behavior of fly ash based geopolymer concrete. *Scientia Iranica*. https://doi.org/10.1016/j.scient.2012.07.006

[23] Raj N, Patil S G and Bhattacharjee B 2014 Concrete mix design by packing density method. *IOSR Journal of Mechanical and Civil Engineering*. https://doi.org/10.9790/1684-11213446

[24] Habibi A, Ramezanianpour A M, Mahdikhani M and Bamshad O 2021 RSM-based evaluation of mechanical and durability properties of recycled aggregate concrete containing GGBFS and silica fume. *Construction and Building Materials* 270: 121431. https://doi.org/10.1016/j.conbuildmat.2020.121431

[25] Romagnoli M, Leonelli C, Kamse E and Lassinantti Gualtieri M 2012 Rheology of geopolymer by DOE approach. *Construction and Building Materials*. https://doi.org/10.1016/j.conbuildmat.2012.04.122

[26] Myers R H, Montgomery D C and Anderson-Cook C M 2016 *Response Surface Methodology: Process and Product Optimization Using Designed Experiments*. 4th edn. Wiley, Hoboken. Retrieved from https://www.wiley.com/en-us/Response+Surface+Methodology%3A+Process+and+Product+Optimization+Using+Designed+Experiments%2C+4th+Edition-p-9781118916018

[27] Kasperkiewicz J 1994 Optimization of concrete mix using a spreadsheet package. *ACI Materials Journal*. https://doi.org/10.14359/1375

[28] Simon M J 2003 *Concrete Mixture Optimization Using Statistical Methods*. *Fhwa-Rd-03-060*, 168

[29] Ahmad S and Alghamdi S A 2014 A statistical approach to optimizing concrete mixture design. *The Scientific World Journal*. https://doi.org/10.1155/2014/561539

[30] Gao Y, Xu J, Luo X, Zhu J and Nie L 2016 Experiment research on mix design and early mechanical performance of alkali-activated slag using response surface methodology (RSM). *Ceramics International*. https://doi.org/10.1016/j.ceramint.2016.04.076

[31] Indian Standard 455 1989 *Portland Slag Cement—Specification* ((R) 1995.). New Delhi: Bureau of Indian Standards. Retrieved from www.bis.org.in

[32] Indian Standard 10289 1987 *Specification for Granualted Slag for the manufacture of Portland Slag Cement* ((R) 1999.). Bureau of Indian Standards, New Delhi. Retrieved from www.bis.org.in

[33] Indian Standard 16714 2018 *Ground Granulated Blast Furnace Slag for Use in Cement, Mortar and Concrete—Specification*. Bureau of Indian Standards, New Delhi. Retrieved from www.bis.org.in

[34] Indian Standard 2720 Part-3/Sec-2 1980 *Methods of test for soils, Part 3: Determination of specific gravity, Section 2: Fine, medium and coarse grained soils* ((R) 2002.). Bureau of Indian Standards, New Delhi. Retrieved from www.bis.org.in

[35] Indian Standard 2386 Part-1 1963 *Methods of Test for Aggregates for Concrete, Part I: Particle Size and Shape* ((R) 2002.). New Delhi: Bureau of Indian Standards. Retrieved from www.bis.org.in

[36] Indian Standard 2386 Part-3 1963 *Methods of test for aggregates for concrete, Part 3: Specific gravity, density, voids, absorption and bulking* ((R) 2002.). New Delhi: Bureau of Indian Standards. Retrieved from www.bis.org.in

[37] Davidovits J 1999 Chemistry of geopolymeric systems, terminology. In: *Second International Conference on Geopolymer*

[38] Davidovits J 2015 False values on CO_2 emission for geopolymer cement/concrete published in scientific papers. The manufacture of geopolymer cement/Concrete, 1–9

[39] Li Q, Cai L, Fu Y, Wang H and Zou Y 2015 Fracture properties and response surface methodology model of alkali-slag concrete under freeze-thaw cycles. *Construction and Building Materials*. https://doi.org/10.1016/j.conbuildmat.2015.06.037

[40] Habibi A, Mohammad A and Mahdikhani M 2021 RSM-based optimized mix design of recycled aggregate concrete containing supplementary cementitious materials based on waste generation and global warming potential resources, conservation and recycling RSM-based optimized mix design of recycled aggregate. *Resources, Conservation & Recycling* 167(April): 105420. https://doi.org/10.1016/j.resconrec.2021.105420

[41] Aziminezhad M, Mahdikhani M and Memarpour M M 2018 RSM-based modeling and optimization of self-consolidating mortar to predict acceptable ranges of rheological properties. *Construction and Building Materials*. https://doi.org/10.1016/j.conbuildmat.2018.09.019

[42] Alyamac K E, Ghafari E and Ince R 2017 Development of eco-efficient self-compacting concrete with waste marble powder using the response surface method. *Journal of Cleaner Production*. https://doi.org/10.1016/j.jclepro.2016.12.156

[43] Bondar D, Nanukuttan S, Provis J L and Soutsos M 2019 Efficient mix design of alkali activated slag concretes based on packing fraction of ingredients and paste thickness. *Journal of Cleaner Production* 218: 438–449. https://doi.org/10.1016/j.jclepro.2019.01.332

[44] Hardjito D, Wallah S E, Sumajouw D M J and Rangan B V 2005 Fly ash-based geopolymer concrete. *Australian Journal of Structural Engineering* 6(1): 77–86. https://doi.org/10.1080/13287982.2005.11464946

[45] Nath P and Sarker P K 2014 Effect of GGBFS on setting, workability and early strength properties of fly ash geopolymer concrete cured in ambient condition. *Construction and Building Materials* 66: 163–171. https://doi.org/10.1016/j.conbuildmat.2014.05.080

[46] Fennis S A A M and Walraven J C 2012 Using particle packing technology for sustainable concrete mixture design. *Heron* 57: 73–102

[47] Soto-Pérez L, López V and Hwang S S 2015 Response Surface Methodology to optimize the cement paste mix design: time-dependent contribution of fly ash and nano-iron oxide as admixtures. *Materials and Design* 86: 22–29. https://doi.org/10.1016/j.matdes.2015.07.049

[48] Cibilakshmi G and Jegan J 2020 A DOE approach to optimize the strength properties of concrete incorporated with different ratios of PVA fibre and nano-Fe_2O_3. *Advanced Composites Letters* 29: 1–16. https://doi.org/10.1177/2633366X20913882

[49] Minitab n.d. *Residual Plots in Minitab—Minitab*. Retrieved July 20, 2022, from https://support.minitab.com/en-us/minitab/18/help-and-how-to/modeling-statistics/regression/supporting-topics/residuals-and-residual-plots/residual-plots-in-minitab/